

Published in final edited form as:

Nat Microbiol. 2017 March 20; 2: 17034. doi:10.1038/nmicrobiol.2017.34.

Guide-independent DNA cleavage by archaeal Argonaute from *Methanocaldococcus jannaschii*

Adrian Zander^{#1}, Sarah Willkomm^{#1}, Sapir Ofer², Marleen van Wolferen³, Luisa Egert¹, Sabine Buchmeier⁴, Sarah Stöckl¹, Philip Tinnfeld⁴, Sabine Schneider⁵, Andreas Klingl⁶, Sonja-Verena Albers³, Finn Werner², Dina Grohmann^{1,*}

¹Department of Microbiology & Archaea Centre, University of Regensburg, Regensburg, 93053, Germany.

²Institute for Structural and Molecular Biology, Division of Biosciences, University College London, London WC1E 6BT, United Kingdom.

³Molecular Biology of Archaea, Institute of Biology II, University of Freiburg, Microbiology, Schaenzlestraße 1, , 79104 Freiburg, Germany.

⁴Institute of Physical and Theoretical Chemistry – NanoBioSciences, Technische Universität Braunschweig-BRICS, Rebenring 56, , 38106 Braunschweig, Germany.

⁵Center for Integrated Protein Science Munich CIPSM, Department of Chemistry, Technische Universität München, Lichtenbergstrasse 4, 85748 Garching, Germany

⁶Biocentre of the LMU Munich, Department Biology I – Plant Development, Großhadernerstr. 2-4, 82152 Planegg-Martinstried, Germany

These authors contributed equally to this work.

Abstract

Prokaryotic Argonaute proteins acquire guide strands derived from invading or mobile genetic elements via an unknown pathway to direct guide-dependent cleavage of foreign DNA. Here, we report that Argonaute from the archaeal organism *Methanocaldococcus jannaschii* (MjAgo) possesses two modes of action: the canonical guide-dependent endonuclease activity and a non-guided DNA endonuclease activity. The latter allows MjAgo to process long double stranded DNAs, including circular plasmid DNAs and genomic DNAs. Degradation of substrates in a guide-independent fashion primes MjAgo for subsequent rounds of DNA cleavage. Chromatinised genomic DNA is resistant to MjAgo degradation and recombinant histones protect DNA from cleavage *in vitro*. Mutational analysis shows that key residues important for guide-dependent target processing are also involved in guide-independent MjAgo function. This is the first-time characterisation of a guide-independent cleavage activity for an Argonaute protein potentially serving as guide biogenesis pathway in a prokaryotic system.

*For correspondence: dina.grohmann@ur.de (DG).

Author Contributions

Conception of the study: DG; experimental work: AZ, SW, MvW, LE, SSt, SO, AK, SB, DG; data analysis: AZ, SW, MvW, SVA, SSchn, DG, AK, FW; writing of the manuscript: DG. All authors edited the manuscript.

Keywords

Argonaute; archaea; DNA-guided gene silencing

Introduction

Argonaute (Ago) proteins are crucially involved in RNA-guided or DNA-guided degradation of target nucleic acids.^{1–3} Present in all three domains of life, they bind short guide strands *in vivo* to target complementary nucleic acids but differ in their substrate specificity. Eukaryotic Agos interact with cytoplasmic RNA substrates 18–23 bp in length^{4–6} while prokaryotic Agos (pAgos) bind and process a variety of substrates ranging from guide DNA/target RNA and guide DNA/target DNA to guide RNA/target DNA.^{7–11} Among them, Ago proteins from the archaeal organisms *Methanocaldococcus jannaschii* (MjAgo), *Pyrococcus furiosus* (PfAgo) and *Natronobacterium gregoryi* (NgAgo) are the only Ago variants that exclusively cleave DNA substrates using a DNA guide *in vitro*.^{7,11–13} Despite the differences in substrate specificity, most Agos investigated so far share a common feature of guide recognition, which is facilitated by a 5'-end phosphate coordinated in the Mid domain binding pocket by conserved amino-acid side chain interactions.^{14–18} One exception are the recently characterized bacterial Ago from *Marinitoga piezophila* (MpAgo) and *Thermotoga profunda* (TpAgo), which specifically recognise RNA guides with a 5'-hydroxyl group.¹⁹ Once Ago is loaded with a guide strand, recognition of partially or fully complementary target nucleic acids via Watson-Crick base pairing is possible. Nucleolytic cleavage of a target strand occurs in case of fully complementary strands with the PIWI domain harbouring the catalytic site. Notably, numerous pAgos, especially short Argonaute variants, have an incomplete catalytic site rendering them inactive.²

While the structural organization of pAgos is well understood, their biological role is still not fully revealed. So far, *in vivo* studies have only been reported for the bacterial organisms *Thermus thermophilus* (Tt) and *Rhodobacter sphaeroides* (Rs). In both cases, Argonaute appears to play a role in host defence.^{8,20} TtAgo acquires short guide DNAs 13–25 nt in length with the canonical phosphate group at the 5'-end. Overexpression of TtAgo leads to the association of TtAgo with short DNA sequences mainly derived from the expression plasmid used to overexpress Ago in *T.thermophilus*.⁸ Guide-associated TtAgo, MpAgo and NgAgo proteins cleave plasmids complementary to the guide DNA by nicking both strands of the plasmid DNA.^{8,19,21} In contrast, RsAgo associates with short guide RNAs 15–19 nt and small complementary DNAs 18–25 nt in length suggesting that RsAgo is involved in RNA-guided DNA silencing.²⁰ The majority of sequences acquired by RsAgo map to genome-encoded foreign nucleic acids like transposons and phage genes.²⁰ RsAgo is a catalytically inactive Ago variant but the operon encoding the Argonaute gene also encodes a nuclease making it feasible that both proteins together mediate RNA-guided silencing in *R. sphaeroides*.

In this study, we describe the guide-independent endonuclease activity of the archaeal MjAgo. We show that MjAgo can process long dsDNAs including plasmids and genomic DNA in the absence of a guide strand. MjAgo-dependent processing of these substrates

leads to the generation of cleavage products potentially suitable as guides. Using these cleavage products in a second cleavage round accelerates processing of the original substrate DNA suggesting that MjAgo can be primed for a second round of cleavage. We furthermore demonstrate that only the chromatinised state of genomic DNA from *M.jannaschii* is protected against MjAgo-mediated degradation, and that histone proteins like A3 are likely to confer this protection. In addition, our structure-based mutational analysis reveals amino acids and structural elements that are of crucial importance for the guide-independent cleavage activity of MjAgo. Taken together, our findings support a scenario in which the non-guided endonuclease activity of MjAgo represents a mechanism to protect a prokaryotic organism against foreign genetic elements.

Results

MjAgo can utilize non-canonical DNA guides for cleavage of DNA targets

First, we were interested to find out which guide length is accepted by MjAgo. Therefore, we initially tested DNA guide strands carrying the canonical 5'-phosphate ranging from 13–23 nt in a guide-dependent target cleavage assay (Figure 1A). Target cleavage required a minimal guide length of 15 nt and MjAgo accepted all guide lengths up to 23 nt (Figure 1B). The number of cleavage products increased with increasing guide length. (We also found efficient cleavage of a non-canonical substrate (41 nt guide / 41 nt target) even if the guide strand does not carry a phosphate group at the 5'-end (Figure 1C,D and S1). None of the substrates was cleaved if the catalytic mutant MjAgo^{E541A} was used (Figure S2). Next, we tested whether MjAgo exhibits orientated loading and cleavage of the 41 nt guide/41 nt target substrate using target strands that either carry the fluorescent label at the 5'-end or towards the 3'-end together with guide strands with and without a 5' phosphate group (Figure 1E). In case of a 5'-phosphorylated 41nt guide, the production of a canonical cleavage product was observed with cleavage occurring opposite nt 10/11 of the guide strand. However, the majority of the substrate is preferentially cleaved from the 5'-end of the target strand in a stepwise manner (Figure 1F). From a structural perspective, it is not feasible that both ends of a 41 nt long guide are accommodated in the Mid and PAZ domain hinting to the possibility that MjAgo is able to bind and process nucleic acids employing a non-canonical mechanism.

MjAgo cleaves long linear and circular double-stranded DNA in a guide-independent fashion

In order to test whether MjAgo also cleaves significantly longer substrates, we incubated MjAgo with dsDNA approximately 750 bp in length and circular double-stranded plasmid DNAs. In both cases, we found cleavage of the substrate in a guide-independent manner if MjAgo wt but not if the catalytic mutant MjAgo^{E541A} is used (Figure 2A,C,D). The DNA is gradually cleaved over time (Figure S3) until final cleavage products smaller than 100 bp accumulate (Figure 2 and 3). Cleavage of long dsDNA by MjAgo is prevented, if EDTA is added (Figure S4). This suggests that the conserved catalytic tetrad, which coordinates two metal ions, is carrying out the cleavage reaction. Degradation occurs quickly at physiological relevant high temperatures of 75°C–85°C but slow degradation takes place at 37°C (Figure 2D).

We attempted to visualise MjAgo associated with long dsDNA fragments (Figure 2B) using transmission electron microscopy (TEM). In the transmission electron micrographs, the MjAgo protein alone, naked linear dsDNA (PCR product) as well as interactions of MjAgo with DNA could be detected. The diameter of the MjAgo protein is approximately 15 to 20 nm, depending on the orientation of the protein.

We successfully detected low levels of MjAgo protein in *M. jannaschii* whole cell lysates using monoclonal anti MjAgo antibodies (Figure S5) indicating that MjAgo is constitutively expressed under normal growth conditions and MjAgo expression does not require external factors that induce MjAgo expression, e.g. infection by a virus or invasion of foreign genetic material. Thus, we were interested to find out whether the genomic DNA (gDNA) of *M. jannaschii* is protected against MjAgo-mediated degradation. MjAgo degrades highly purified “naked” gDNA while chromatinised DNA is resistant to degradation (Figure 2E). In order to investigate whether the abundant A3 histone from *M. jannaschii* is the agent that confers Ago resistance, we reconstituted recombinant histone A3 from *M. jannaschii* with a short dsDNA (750 bp) DNA template to enable the formation of histone-DNA complexes. The latter were not significantly degraded by MjAgo (Figure 2F) indicating that histone-bound DNA is not accessible for MjAgo or that the histones induce a DNA conformation that prevents MjAgo association with the DNA. Interestingly, when low amounts of A3 are added, DNA becomes accessible for MjAgo leading to a ladder-like degradation pattern reminiscent of patterns created by digestion of chromatin with the enzyme Micrococcal nuclease (MNase) (Figure S6).

Recently, it was shown that genomic DNA from archaeal species exhibit different methylation patterns.²² Therefore, we were interested to find out whether methylation signatures serve as recognition sites for MjAgo cleavage specificity as some nucleases show reduced or no activity on methylated substrates.²³ Genomic DNA from *M. jannaschii* and *P. furiosus* carry a m4C, m6A, m5C methylation, whereas gDNA from *S. acidocaldarius* is only methylated at position 4C and 5C. Genomic DNA from *P. furiosus* and *S. acidocaldarius* were also degraded by MjAgo indicating that different methylation patterns do not influence the cleavage activity of MjAgo (Figure S7). Additionally, we used bacterial-purified plasmids that carried either the dam or the dcm methylation or both. All plasmids were degraded by MjAgo indicating that the known bacterial methylation patterns do not influence MjAgo activity (Supplementary Figure 7).

Next, we determined the size of the final degradation product. To this end, we radiolabelled final cleavage products (Figure 3A) at the 5'-end with ³²P-phosphate with or without prior removal of a 5'-terminal phosphate group by alkaline phosphatase (AP) treatment and analysed the length distribution on a denaturing sequencing gel (Figure 3B). Nucleolytic degradation of dsDNA by MjAgo yielded mainly final products in the range of 8-13 nt with weak bands visible for longer products (14 to approximately 17 nt). Radiolabelling was also successful when samples without AP treatment were used suggesting that MjAgo creates short DNA fragments that either do or do not carry a 5'-terminal phosphate group. Cleavage assays using a canonical substrate showed that unphosphorylated guides can also direct cleavage of a target (Figure S8).

We tested whether these DNA fragments can serve as guides to allow sequence-specific degradation in a subsequent round of plasmid cleavage. Plasmid DNA degradation is significantly accelerated if the reaction is supplemented with the final reaction products of a previous cleavage reaction using the same plasmid (Figure 3C). In case a plasmid unrelated in sequence is used, the cleavage reaction appears to be faster as compared to a reaction without pre-digestion of a prior plasmid but is still significantly slower as compared to the reaction with pre-digestion of the same plasmid. Association of MjAgo with short DNA guides that accumulate during the first round of plasmid degradation leading to cleavage of a plasmid with the same sequence might represent one component of a priming mechanism. However, a second unknown factor seems to play a role as a plasmid unrelated in sequence is apparently also faster processed as compared to a reaction without a pre-digestion step. Nevertheless, this accelerated reaction is still significantly slower in comparison to a reaction where the exact same plasmid for the first and second round of digestion was used. Possibly, one round of MjAgo-mediated cleavage during the pre-digestion of a plasmid induces a cleavage-competent conformational state that leads to a fast processing of substrates in general.

Next, we analysed whether canonical 5'-phosphorylated guide strands (21 nt) direct specific nicking and linearization of a plasmid as it has been demonstrated for other prokaryotic Argonaute proteins.^{8,19,21} However, no specific band indicative for nicking or linearization of the plasmid was observed (Figure 3D).

Mutational analysis of MjAgo-mediated non-canonical DNA substrate cleavage

In order to identify the structural elements that are important for the guide-independent activity of MjAgo, we carried out a mutational analysis. MjAgo anchors the 5'- and 3'-end of a canonical guide strand in dedicated binding pockets in the Mid and PAZ domain respectively (PDB: 5G5S and 5G5T).^{1,24} We tested whether mutations in the functional domains of MjAgo (Figure 4A) affect the plasmid cleavage activity of MjAgo. PAZ binding pocket mutants (Y194A, H123A, Y217A, E246A) showed significantly reduced cleavage activity (Figure 4B) suggesting that the interaction between DNA and the PAZ domain is important for the guide-independent cleavage activity. The PAZ domain undergoes a conformational transition upon loading of the guide DNA (Figure S9).²⁴ In the apo enzyme, residues N170 (PAZ domain) and D438 (Mid domain) are in close proximity potentially stabilising the closed conformation of apo MjAgo (Figure 4A, inset). We mutated position N170 and found that the mutant was active suggesting that an interruption of the putative N170-D438 interaction does not influence MjAgo's guide-independent cleavage activity. Additionally, we tested MjAgo variants with mutations in helix 8 (L270P and W274V). Helix 8 corresponds to helix 7 in hAgo2, which is a mobile element important for efficient formation of the guide/target duplex.^{15,18,24,25} Helix 8 mutations were active albeit with slightly reduced cleavage activity. Mutations of amino acids lining a putative secondary nucleic acid binding channel (F572A, Q574A, N575A), a feature we recently identified in the crystal structures of MjAgo (PDB: 5G5T)²⁴ (Figure S10), did not significantly reduce cleavage activity. Only the mutant F572A showed a slightly reduced activity, which might be due to the close proximity of this residue to the active site. We furthermore tested mutations of amino acids that are directly involved in the coordination of the 5'-end of a

conventional guide (K435A, D438P, Q457A, N458A, Q479A, K483A). Only the D438 and K483A mutants were completely inactive or strongly reduced in activity.

Among these mutants, only mutation of residues Y194, E246 and K483 seem to be critical for both modes of MjAgo activity. Lysine 483 is involved in the coordination of a magnesium ion in the Mid binding pocket, which seems of crucial importance for MjAgo activity. Interestingly, residues Q457, N458, L270P, F572, Q574 and N575 are important for the guide-dependent but not guide-independent cleavage activity as all of these mutants are catalytically inactive using a canonical substrate.²⁴

MjAgo associates with small DNA *in vivo* and impairs growth in a heterologous archaeal expression system

Having established that MjAgo is able to process genomic DNA from foreign species *in vitro*, we next tested whether cleavage of DNA occurs also *in vivo* and affects the viability of the organism used for heterologous expression of MjAgo. We transformed suitable expression plasmids encoding either the wildtype MjAgo or the catalytically inactive mutant into *S. acidocaldarius* and *E. coli*. We expressed and purified the recombinant MjAgo from *E. coli* lysate via affinity chromatography and subsequently isolated nucleic acids associated with MjAgo (nucleic acids remain bound to MjAgo if the extraction and purification is carried out at 4°C but not if carried out at room temperature). These nucleic acids are smaller than 100 bases and resistant to RNases but sensitive to DNase treatment (Figure 3E) suggesting that MjAgo interacts with short DNAs *in vivo* in the heterologous expression host *E. coli*. These DNAs might represent MjAgo degradation products. However, growth of bacteria was not impaired by overexpression of MjAgo, most likely because DNA replication is an extremely fast process in *E. coli* but the guide-independent cleavage activity of MjAgo is very slow at 37°C. In order to exclude the possibility that traces of these short nucleic acids remain bound to MjAgo during protein preparation at room temperature and serve as guides, we purified MjAgo associated nucleic acids and added them back to a reaction containing MjAgo and plasmid DNA at defined concentrations (Figure S11). In case these DNAs (unrelated in sequence to the plasmid DNA used for the plasmid cleavage assay) serve as unspecific guides for MjAgo, an acceleration of the cleavage reaction should be observed. However, the presence of these short DNAs (Figure S11A) did neither influence nor stimulate the MjAgo mediated cleavage of plasmid DNA even at high concentrations (Figure S11B). Consequently, the MjAgo activity is genuinely a guide-independent activity.

Since no genetic system is established for *M. jannaschii*, we were not able to affinity-purify endogenous MjAgo and to isolate nucleic acids associated with MjAgo *in vivo*. However, *S. acidocaldarius* is a genetically tractable archaeal organisms that does not encode an Argonaute variant but – like *M. jannaschii* – is a thermophile with a comparable optimal growth temperature (70-80°C). Thus, using *S. acidocaldarius* as heterologous expression host, we were able to study MjAgo activity in an archaeal organism at near optimal temperatures. We found approximately 25-fold less transformants when using a plasmid encoding wildtype MjAgo as compared to the catalytically inactive mutant (wt MjAgo: 13 colonies vs MjAgo^{E541A}: 341 colonies) for transformation. In order to verify that MjAgo

is expressed in these cells, we carried out MjAgo immunodetection in whole cell extracts. While we found good expression levels of MjAgo in case of the catalytic mutant, almost no MjAgo was detectable in case of the transformants that carried the expression plasmid for the wildtype MjAgo (Figure S12A/B). In order to find out whether the reduced protein level is due to proteolytic degradation of wt MjAgo or reduced plasmids levels in the cells, we PCR-amplified the expression plasmid and found reduced levels of the MjAgo wt expression plasmid as compared to the plasmid levels of the catalytic mutant in the cell lysate (Figure S12C). These results suggest that MjAgo is active when expressed in the crenarchaeal organism *S. acidocaldarius* and that active MjAgo negatively affects the viability of the organism possibly due to the MjAgo-mediated degradation of *Sulfolobus*’ gDNA. Note that in contrast to *M. jannaschii*, *Sulfolobus* does not encode histone but histone-like proteins (e.g. Alba, Cren7 and Sul7) that decorate the genomic DNA and compact the genome for example via loop formation. However, the interaction of Alba is less stable than the tight wrapping of DNA in nucleosomes most likely leaving the genomic DNA more susceptible for MjAgo action.²⁶

Discussion

Prokaryotic Agos are able to use short DNA or RNA guides to direct guide-dependent plasmid nicking or double-strand cleavage of plasmid DNA at a single site. Here, we show that the archaeal Argonaute from *M. jannaschii* works as both, a guided and guide-independent endonuclease. The guide-independent endonuclease activity allows the processing of non-canonical substrates like linear and circular dsDNAs representing an Argonaute function that potentially drives silencing of invading and self-replicating genetic elements.

Testing the substrate spectrum of MjAgo revealed that MjAgo requires a minimal guide length of 15 nt for its guide-dependent DNA cleavage activity and cleavage is most efficient with a guide length of 19 nt. This is in good agreement with other prokaryotic Agos that utilise guides in the size range of 14-25 nt.^{7,8,12,19-21} Base pairing of a 14-15 nt guide with a target appears to be the minimally required length in all the characterised pAgos that yields a stable duplex even at the high reaction temperatures typical for thermophiles. The stability of the duplex must be enhanced beyond the thermal stability of the dsDNA by the intricate network of interactions in the Mid binding pocket and the seed region of the guide to ensure that the substrate remains hybridised during a single round of target cleavage. We additionally observed usage of guides well above the canonical guide lengths (e.g. using a 41 nt guide), which has also been reported recently for MpAgo.¹⁹ Structural studies showed that the 5’- and 3’-end of the guide is anchored in the Mid and PAZ binding pocket, respectively.^{16,19,21} The 3’-end is released from the PAZ domain upon target loading.^{10,11} In case of a 41 nt guide, sterical constraints would not allow the docking of the 5’- and the 3’-end in the binding pockets. We found that the 41 nt guide is nevertheless associated with the Mid domain pocket when a 5’-phosphate is present as the canonical cleavage product is observed. This reaction competes with a cleavage reaction that preferentially starts from the 3’-end of the guide and leads stepwise processing of the target. Cleavage leads to the generation of a new phosphate group that could direct the subsequent cleavage reaction that can occur on both strands resulting in an apparent stepwise degradation of

the labelled target. However, the 3'-end cleavage mode is slower than the phosphate-guided reaction suggesting that the substrate is not ideally positioned for efficient cleavage in the Mid domain binding pocket. Interestingly, hAgo2 is also capable to process non-canonical long dsRNAs. Cheloufi *et al* showed that hAgo2 degrades the 41 nt long pre-miRNA-451 in a Dicer-independent manner.²⁷ hAgo2 cleaves this substrate at the canonical cleavage site suggesting that the 5'-end of the dsRNA is anchored in the Mid domain and hAgo2 is able to accommodate this species without an interaction of the 3'-end and the PAZ domain.

A gradual degradation is also observed when long dsDNA, plasmid DNA or genomic DNA is processed by MjAgo. Although a preferential association of MjAgo with the terminus of a long dsDNA is not detectable in the EM images, it is still evident that MjAgo is associated with dsDNA and might employ a comparable sliding mechanism as described for hAgo2 to search for the terminus of the DNA.²⁸ In case of circular DNA, first, cleavage of both strands has to occur to result in the observed linearized form of the plasmid. This step appears to be more efficient at elevated temperatures. Here, thermal breathing of the DNA (especially in AT-rich stretches) is enhanced resulting in transiently opened DNA that could serve as entry point for MjAgo. Nicking of one of the strands results again in a free phosphate group at the terminus of the DNA, which can be positioned in the Mid binding pocket followed by cleavage of the second strand in close proximity that is detectable as linearized plasmid. The mutational analysis underscores the importance of the magnesium in the Mid binding pocket as mutations of residues 483 that is involved in the coordination of the magnesium and the terminal base leads to strongly reduced plasmid degradation activity. Equally important is D438, which is part of the so-called nucleotide-specificity loop – a conserved feature for the coordination of the 5'-end terminal nucleotide.¹⁷ In MjAgo, D438 is part of a 3¹⁰ helix that forms upon formation of the binary guide-MjAgo complex.²⁴ Interruption of this helix reduces both, the guide-dependent and guide-independent MjAgo activity. The mutational analysis also revealed that the PAZ domain is critical for MjAgo-mediated plasmid degradation. Even though the long substrates cannot be anchored in both, the Mid and PAZ binding, the PAZ domain has a general affinity for nucleic acids.¹⁶ In fact, all pAgos that show guide-dependent plasmid DNA cleavage have to accommodate at least three nucleic acid strands in the protein. So far, no structural or mechanistic insights are available that shed light on the question of substrate accommodation in case of plasmid processing by pAgos. Structural data showed, that in addition to the Mid and PAZ domain, a second positively charged nucleic acid binding channel (Figure S10) is important for the efficient guide-dependent DNA endonuclease activity of MjAgo.²⁴ This channel might provide space for one of the DNA strands handled by MjAgo during plasmid processing. Based on structural studies, it has been proposed that the channel formed in between the PAZ- and N-terminal domain accommodates the target strand.²⁹ It would be conceivable that in MjAgo a strand separation is achieved by guiding one of the DNA strands through the primary (PAZ/N-terminal cleft) and secondary DNA binding channel (PIWI/N-terminal tunnel) with strand annealing after both strands have passed the N-terminal domain. Mutational analysis of residues lining this putative secondary binding channel did not reveal whether this channel might be a structural feature important for guide-independent cleavage of long dsDNA substrates by MjAgo. Recently, the structure of RsAgo in complex with a guide and target strand has been solved.²¹

Here, base pairing of the guide/target duplex was not interrupted in the 3'-prime region of the guide but maintained up to nucleotide 18 due to a slightly altered orientation of the N-terminal domain ('packing-type' N-terminal domain). In structures of substrate-associated TtAgo, the guide and target strand is separated after nucleotide 16 by the action of the N-terminal domain ('wedge-type' N-terminal domain).^{10,30} This example demonstrates that substrate positioning in prokaryotic Ago variants does not follow a conserved pathway and MjAgo might bind nucleic acids in yet another slightly different configuration. A secondary DNA binding channel has not been identified in other pAgos yet rendering MjAgo the only characterised Ago variant so far that possesses additional structural features, possibly required to allow for the non-guided DNA endonuclease activity (Figure S13).

Taken together, a picture of the *in vivo* function of MjAgo emerges (Figure 5A). MjAgo might serve as a safeguard system that, upon invasion of foreign nucleic acids like plasmids or viral DNA, is able to degrade these DNAs in a non-specific fashion via the guide-independent endonuclease function. The circular 1.7 Mb genome and the two extrachromosomal elements of *M. jannaschii* are inert against Ago action, likely because histones such as A3 intimately interact with the DNA and thus deny Ago access. In conjunction with the data collected from heterologous expression of MjAgo in *S. acidocaldarius*, an organism which does not encode any histones, these results lead to the hypothesis that the chromatinisation state of the DNA would serve a "self vs non-self" discrimination marker. This wave of defence is relatively slow but followed by a faster phase. Potentially, guides are recruited during the first step of guide-independent MjAgo action priming MjAgo for a second round of guide-dependent cleavage with significantly increased substrate turnover. In contrast to the CRISPR-Cas systems, the postulated MjAgo-mediated defence system does not possess a memory. Earlier experiments showed that guide strands dissociate from MjAgo¹¹, which ultimately allows re-priming of the cellular MjAgo pool. Interestingly, Ago from *P. furiosus*, does not exhibit complete degradation but only linearization of plasmid DNA in a guide-independent manner⁷ even though *P. furiosus* also contains chromatinised DNA. The genomic context of the MjAgo gene (Figure 5B) also hints to the possibility that MjAgo is involved in DNA repair and/or recombination processes and its catalytic activity might be regulated by so far unknown proteins.

Even though guide sequences derived from exogenous plasmids, transposable elements and cellular transcripts were found to be associated with TtAgo and RsAgo *in vivo*, the biology of guide strand generation remained elusive as no pre-processing enzyme comparable to the eukaryotic Dicer nuclease could be identified so far that might fulfil this function. The non-canonical substrate usage of MjAgo provides a first mechanistic rationale how Ago can be primed in prokaryotic organisms. However, in other prokaryotes a different mechanism seems to be in place. They remain to be identified, since to date no guide-independent endonucleolytic degradation of plasmid DNA was demonstrated for other guide-dependent DNA-silencing enzymes including TtAgo, NgAgo, MpAgo, PfAgo and RsAgo.

Methods

Protein preparation

Recombinant Argonaute from *M. jannaschii* was produced as described previously.¹¹ In brief, MjAgo was expressed in *E. coli* Rosetta(DE3)pLysS cells (Novagen). Cells were grown for 16h at 37°C after induction of expression with 1 mM IPTG. After harvesting the cells by centrifugation (8000 g, 20 min) the cells were resuspended in resuspension buffer (50 mM Tris/HCl pH 7.4, 100 mM NaCl, 1 mM MgCl₂, 10% glycerol, 20 mM Imidazol). Cells were lysed by sonification. A heat treatment step (30 min at 85 °C) followed by centrifugation for 45 min at 15.000 g leads to a pre-purification of the heat stable recombinant MjAgo, which was found in the soluble fraction and was further purified by affinity chromatography using a HisTrap column (GE Healthcare). The protein was eluted in a buffer containing 50 mM Tris/HCl pH 7.4, 100 mM NaCl, 1 mM MgCl₂, 10% glycerol, 250 mM imidazol.

For the production of the catalytic mutant MjAgo^{E541A}, the MjAgo gene was mutated to introduce an Alanine codon at position E541 using the QuikChange II site-directed mutagenesis kit (Agilent). The recombinant protein was produced in *E. coli* Rosetta(DE3)pLysS cells and extraction of the mutated MjAgo protein was performed as described for the wild-type protein with the exception that the heat treatment step was carried out at 75°C for 30 min. All other mutants were generated using the QuikChange II site-directed mutagenesis kit (Agilent), expressed in *E. coli* Rosetta(DE3)pLysS (50 ml expression cultures) as described for the MjAgo wildtype including a heat treatment step for 30 min at 85°C. MjAgo mutants were purified using Ni-NTA spin columns (Qiagen) according to manufacturer's instructions. Proteins were eluted in the same elution buffer as described for large scale purification via the HisTrap column.

Cloning and preparation of histone A3 from *Methanocaldococcus jannaschii*

The gene encoding *M. jannaschii* histone A3 was cloned from genomic DNA using PCR. Following PCR amplification, cloning into pGEM-T (Promega) and sequence verification, the A3 insert was subcloned into the expression vector pET21a(+) (Novagen) using NdeI and XhoI restriction sites. The resulting pET-A3 vector was transformed into the Rosetta2 expression strain (Novagen), grown in rich media supplemented with ampicillin (100 µg/ml) and induced with 1 mM IPTG for 3 hours. The expression culture was harvested by centrifugation and soluble proteins extracted in N100 extraction buffer (100 mM NaCl, 25 mM Tris-acetate pH 8.0, 10 mM MgCl₂, 1 mM DTT) supplemented with EDTA-free protease inhibitor cocktail (Roche) by using a cell press in the presence of 20 µl DNaseI (2500 U/ml) and 20 µl RNase (10 mg/ml). The extract was centrifuged for 30 minutes at 15000 g at 4 °C to remove cell debris. The cleared lysate was heat treated at 70 °C for 30 minutes followed by centrifugation at 13,000 g for 30 minutes at 4 °C to remove denatured *E. coli* proteins. The supernatant was loaded onto a 1 ml heparin column (HiTrap Heparin HP, GE Healthcare) equilibrated with N100. The protein was eluted with a linear gradient from 0-1.0 M NaCl over 10 CV using N1000 buffer (N100-like buffer containing 1,000 mM NaCl). Fractions containing A3 were pooled and dialyzed (Slide-A-Lyzer Dialysis Cassettes, Life technologies) into N250 buffer (N100-like containing 250 mM NaCl).

Synthetic oligonucleotides and DNAs

DNA guide and target sequences of the let-7 based 20/21mer substrate are listed in Figure 1A. The sequences of the 41 nt long DNA substrate is as follows:

41 nt guide: 5'-ACGGACATTACGAGGTAGTAGGTTGTATAGTCTTATCACCT

41 nt target: 5'-AGGTGATAAGACTATACAACCTACTACCTCGTAATGTCCGT.

All oligonucleotides were HPLC-purified and purchased from MWG (Ebersberg, Germany).

Plasmid DNA used for MjAgo activity assays throughout this work were either standard pGEX-2TK or pET21(a) based vectors. Plasmid DNA was purified from *E. coli* DH5 α cells using the HiSpeed Plasmid Midi Kit (Qiagen).

Genomic DNA from *M. jannaschii* was prepared using the DNeasy Blood and Tissue Kit (Qiagen) followed by RNase digestion (Thermo Scientific) of remaining tRNA and rRNA. Genomic DNA from *P. furiosus* was kindly provided by Winfried Hausner (Institute for Microbiology and Archaea Centre, University Regensburg). Genomic DNA from *S. acidocaldarius* was prepared using the Genelute™ Bacterial genome DNA kit (Sigma).

Purification of chromatin from *M. jannaschii* biomass

1 g *M. jannaschii* biomass ($\sim 7 \times 10^9$ cells/g) was resuspended in 20 ml PBS (including protease inhibitor cocktail, Roche) and centrifuged at low speed at 1,500 g for 10 minutes at 4°C to remove black residue from the culture medium (mostly FeS). The supernatant was transferred to a new tube and, if necessary, the wash step repeated 2-3 x until the pellet has a white appearance. The supernatant was centrifuged at high speed at 14,000 g for 10 minutes at 4°C in order to pellet the cells. After removal of the supernatant, the cell pellet was carefully resuspended by pipetting in 5 ml chromatin extraction buffer (25 mM HEPES pH 7, 15 mM MgCl₂, 100 mM NaCl, 400 mM sorbitol and 0.5 % Triton X-100). The chromatin extract was incubated for 30 minutes at 4°C and aliquoted into 100 μ l portions. Following centrifugation at 14,000 g for 15 minutes at 4 °C, the supernatant was removed and the chromatin pellet resuspended in 50 μ l extraction buffer, snapfrozen in liquid Nitrogen and stored at -80° C.

Activity assays

DNA-guided cleavage assays were performed by combining 3 μ M recombinant MjAgo with 0.33 μ M guide DNA and 0.67 μ M target DNA in a buffer containing 50 mM Tris/HCl pH 7.4, 100 mM NaCl, 5 mM MgCl₂, 2% glycerol, 10 mM DTT, and 67 μ g/ml BSA in a total volume of 15 μ l. The target DNA and the resulting cleavage products are detected via the fluorescent signal of the coupled fluorophore (see Figures for coupling sites). All components were combined at room temperature and the enzymatic reaction was initiated by incubating the samples at 85 °C. 10 μ l of the reactions were stopped by the addition of 10 μ l formamide-loading buffer and the resulting fragments were separated on a 12% denaturing polyacrylamide gel for 80 min at 70W. The fluorescent signal was visualised using a FLA7000 scanner (GE Healthcare).

Cleavage assays using a dsDNA PCR fragment, circular plasmid DNA (pGEX-2TK vector) or genomic DNA was performed in a buffer containing 50 mM Tris/HCl pH 7.4, 100 mM NaCl, 5 mM MgCl₂, 2% glycerol, 10 mM DTT, and 67 µg/ml BSA in a total volume of 10 µl. If not noted otherwise reactions contained 1 µM MjAgo. DNA concentrations are given in the figure legends. Samples were incubated at 37°C, 75°C or 85°C (see figure legends). Reactions including the catalytic mutant were incubated at 75°C due to the reduced heat stability of the mutated protein. Reactions were stopped at the given time points (see figure legends) by the addition of 1 volume 6M urea and incubation for 5 min at 85°C.

1 µl of Green Buffer (Thermo Fisher, Fast Digest Kit) was added prior to analysis of the sample using agarose gel electrophoresis. For guide-dependent plasmid cleavage reactions a pET21(a) plasmid was used and two matching standard guide sequences were designed that target each strand of the T7 promoter sequence encoded in the pET21 plasmid (T7 fw guide: 5'-PHO-CCCTATAGTGAGTCGTATTA, T7 rev guide: 5'-PHO-CTCACAATTCCCCCATAGTG). Samples were incubated for 5 min at 85°C prior to separation and analysis via agarose gel electrophoresis (1xTAE running buffer including 1 M urea in the buffer and gel).

For MjAgo-mediated cleavage assays that included the histone A3, 14.3 µM histone A3 was pre-incubated with 1.5 µg dsDNA (PCR fragment, 750 bp) in 50 mM Tris/HCl pH 7.4, 100 mM NaCl, 5 mM MgCl₂, 2% glycerol, 10 mM DTT, and 67 µg/ml BSA for 10 min at 65°C. Subsequently, 1 µM MjAgo was added and the sample incubated at 85°C (see figure legends for incubation times). Reaction were stopped by fast cooling to 4°C followed by purification of the DNA using the PCR purification kit from Qiagen. Samples were incubated for 5 min at 85°C prior to separation and analysis via agarose gel electrophoresis (1xTAE running buffer).

Isolation and radiolabelling of DNA degradation products after MjAgo-mediated plasmid digestion

Plasmid DNA digest was conducted as described above. One part of the degraded DNA was 5'-dephosphorylated using Antarctic phosphatase (NEB) and purified via Sephadex-G50 columns (GE Healthcare) to remove excess phosphate. Subsequently, dephosphorylated as well as untreated samples of the plasmid DNA fragments were radioactively labelled with [γ -³²P] ATP (Perkin Elmer) using T4 PNK (Thermo Fisher Scientific). Modified DNA fragments were purified from excess [γ -³²P] ATP using Sephadex G50 columns (GE Healthcare). Labelling success was controlled using liquid scintillation counting. A radioactively labelled size marker was created by digesting RNA (5'-GCC UCA GCA CGU AAC UCU ATT-3') carrying a radioactive 5'-phosphate using RNase T1 (Thermo Fisher Scientific). Samples were adjusted to equal counts according to liquid scintillation counting, mixed with 1 volume loading buffer (95% formamide, 0.025 % (w/v) SDS, 0.025 % bromophenolblue, 0.025 % xylene cyanol, 0.5 mM EDTA) and analysed using 20 % denaturing PAGE followed by autoradiography.

Heterologous expression of MjAgo in *Sulfolobus acidocaldarius*

S. acidocaldarius MW001³¹ was grown aerobically at 75°C in basal Brock medium³², supplemented with 0.1% NZ amine, 0.2% dextrin and 20 µg/ml uracil and adjusted to pH 3.5 with sulfuric acid. For solid media the medium was supplemented with 6 mM CaCl₂ and 20 mM MgCl₂ and 1.2% gelrite. Plates were incubated for 6 days at 75°C. To express MjAgo in *S. acidocaldarius*, expression plasmids were constructed by cloning the gene encoding MjAgo (*MJ_1321*) into shuttle vector pSVA1551 (Wagner and Albers, unpublished). The latter is a modified derivative of pCmalLacS³³. To create a catalytically inactive mutant of MjAgo, pSVA1551-MjAgo was mutated using site-directed mutagenesis, introducing an E541A mutation. The plasmids were transformed into *S. acidocaldarius* MW001 as described previously³⁴. Transformants were grown in 50 ml Brock medium³² supplemented with 0.2% NZ-amine to an OD₆₀₀ of around 0.5. Expression was induced by adding 0.4% maltose and incubating the cells for four more hours at 75°C.

To determine the plasmid-sequences of *MJ_1321* in the expression cultures, a PCR was performed on the lysates using MjAgo specific primers³⁴. The PCR product was sequenced using the following primers:

MjAgo fw: 5'-CACCATGGTTTTAAATAAAGTTACATATAAAATAAATGC

MJ_1321_internal_1: 5'- CACTGGTTGATGCTCCAAAC

MJ_1321_internal_2: 5'- TGGGACTTGACACTGGATTG

MJ_1321_internal_3: 5' – TACTCCTCTAATAGTGCTTTATC

MjAgo rev: 5' - TTATATGAAATATAAGAATCCATGC

TEM analysis of MjAgo-DNA complexes

A purified and concentrated solution of MjAgo or MjAgo-DNA complexes (5 µl) was applied to glow-discharged carbon-coated copper grids, washed 2 to 5 times with double distilled water, shortly blotted onto filter paper after each step and negative-stained with 2 % (w/v) uranyl acetate for 20 s³⁵. Afterwards, the grids were blotted on filter paper again and air dried for subsequent transmission electron microscopy (TEM). For this, we used a Zeiss EM 912 in combination with an integrated OMEGA energy filter and operated at 80 kV in the zero-loss mode.

Acknowledgments

We would like to acknowledge all members of the Grohmann lab and in particular Kevin Kramm for cloning of the MjAgo catalytic mutant. We would like to thank Gunter Meister for fruitful discussions. Work in the Grohmann RNAP laboratory was funded by the Deutsche Forschungsgemeinschaft (GR 3840/2-1). SVA and MvW acknowledge funding by the European Research Council (starting Grant ARCHAELLUM 311523). S. Schn. acknowledges funding by the Deutsche Forschungsgemeinschaft, the excellence cluster CIPSM and Fonds der Chemischen Industrie.

Data availability

Primary accession: PDB data bank: 5G5S, 5G5T. All other data that support the findings of this study are available from the corresponding authors upon request.

References

1. Willkomm S, Zander A, Gust A, Grohmann D. A prokaryotic twist on argonaute function. *Life*. 2015; 5: 538–53. DOI: 10.3390/life5010538 [PubMed: 25692904]
2. Swarts DC, et al. The evolutionary journey of Argonaute proteins. *Nature structural & molecular biology*. 2014; 21: 743–53. DOI: 10.1038/nsmb.2879 [PubMed: 25192263]
3. Meister G. Argonaute proteins: functional insights and emerging roles. *Nature reviews Genetics*. 2013; 14: 447–59. [PubMed: 23732335]
4. Elbashir SM, et al. Duplexes of 21-nucleotide RNAs mediate RNA interference in cultured mammalian cells. *Nature*. 2001; 411: 494–8. [PubMed: 11373684]
5. Elbashir SM, Lendeckel W, Tuschl T. RNA interference is mediated by 21- and 22-nucleotide RNAs. *Genes & development*. 2001; 15: 188–200. DOI: 10.1101/gad.862301 [PubMed: 11157775]
6. Zamore PD, Tuschl T, Sharp PA, Bartel DP. RNAi: double-stranded RNA directs the ATP-dependent cleavage of mRNA at 21 to 23 nucleotide intervals. *Cell*. 2000; 101: 25–33. [PubMed: 10778853]
7. Swarts DC, et al. Argonaute of the archaeon *Pyrococcus furiosus* is a DNA-guided nuclease that targets cognate DNA. *Nucleic acids research*. 2015; 43: 5120–9. DOI: 10.1093/nar/gkv415 [PubMed: 25925567]
8. Swarts DC, et al. DNA-guided DNA interference by a prokaryotic Argonaute. *Nature*. 2014; 507: 258–61. DOI: 10.1038/nature12971 [PubMed: 24531762]
9. Wang Y, et al. Structure of an argonaute silencing complex with a seed-containing guide DNA and target RNA duplex. *Nature*. 2008; 456: 921–6. DOI: 10.1038/nature07666 [PubMed: 19092929]
10. Wang Y, et al. Nucleation, propagation and cleavage of target RNAs in Ago silencing complexes. *Nature*. 2009; 461: 754–61. DOI: 10.1038/nature08434 [PubMed: 19812667]
11. Zander A, Holzmeister P, Klose D, Tinnefeld P, Grohmann D. Single-molecule FRET supports the two-state model of Argonaute action. *RNA biology*. 2014; 11: 45–56. DOI: 10.4161/rna.27446 [PubMed: 24442234]
12. Gao F, Shen XZ, Jiang F, Wu Y, Han C. DNA-guided genome editing using the *Natronobacterium gregoryi* Argonaute. *Nature biotechnology*. 2016. [PubMed: 27136078]
13. Willkomm S, Zander A, Grohmann D, Restle T. Mechanistic Insights into Archaeal and Human Argonaute Substrate Binding and Cleavage Properties. *PloS one*. 2016; 11 e0164695 doi: 10.1371/journal.pone.0164695 [PubMed: 27741323]
14. Ma JB, et al. Structural basis for 5'-end-specific recognition of guide RNA by the *A. fulgidus* Piwi protein. *Nature*. 2005; 434: 666–70. DOI: 10.1038/nature03514 [PubMed: 15800629]
15. Schirle NT, MacRae IJ. The crystal structure of human Argonaute2. *Science*. 2012; 336: 1037–40. DOI: 10.1126/science.1221551 [PubMed: 22539551]
16. Wang Y, Sheng G, Juranek S, Tuschl T, Patel DJ. Structure of the guide-strand-containing argonaute silencing complex. *Nature*. 2008; 456: 209–13. DOI: 10.1038/nature07315 [PubMed: 18754009]
17. Frank F, Sonenberg N, Nagar B. Structural basis for 5'-nucleotide base-specific recognition of guide RNA by human AGO2. *Nature*. 2010; 465: 818–22. [PubMed: 20505670]
18. Nakanishi K, Weinberg DE, Bartel DP, Patel DJ. Structure of yeast Argonaute with guide RNA. *Nature*. 2012; 486: 368–74. DOI: 10.1038/nature11211 [PubMed: 22722195]
19. Kaya E, et al. A bacterial Argonaute with noncanonical guide RNA specificity. *Proceedings of the National Academy of Sciences of the United States of America*. 2016; doi: 10.1073/pnas.1524385113 [PubMed: 27035975]
20. Olovnikov I, Chan K, Sachidanandam R, Newman DK, Aravin AA. Bacterial argonaute samples the transcriptome to identify foreign DNA. *Molecular cell*. 2013; 51: 594–605. DOI: 10.1016/j.molcel.2013.08.014 [PubMed: 24034694]

21. Miyoshi T, Ito K, Murakami R, Uchiumi T. Structural basis for the recognition of guide RNA and target DNA heteroduplex by Argonaute. *Nature communications*. 2016; 7 11846 doi: 10.1038/ncomms11846 [PubMed: 27325485]
22. Blow MJ, et al. The Epigenomic Landscape of Prokaryotes. *PLoS genetics*. 2016; 12 e1005854 doi: 10.1371/journal.pgen.1005854 [PubMed: 26870957]
23. Loenen WA, Dryden DT, Raleigh EA, Wilson GG, Murray NE. Highlights of the DNA cutters: a short history of the restriction enzymes. *Nucleic acids research*. 2014; 42: 3–19. DOI: 10.1093/nar/gkt990 [PubMed: 24141096]
24. Willkomm S, Oellig CA, Zander A, Restle T, Keegan R, Grohmann D, Schneider S. Structural and mechanistic insights into an archaeal DNA-guided Argonaute protein. under consideration for back-to-back publication in *Nature Microbiology*. 2016. [PubMed: 28319084]
25. Elkayam E, et al. The structure of human argonaute-2 in complex with miR-20a. *Cell*. 2012; 150: 100–10. DOI: 10.1016/j.cell.2012.05.017 [PubMed: 22682761]
26. Peeters E, Driessen RP, Werner F, Dame RT. The interplay between nucleoid organization and transcription in archaeal genomes. *Nature reviews Microbiology*. 2015; 13: 333–41. [PubMed: 25944489]
27. Cheloufi S, Dos Santos CO, Chong MM, Hannon GJ. A dicer-independent miRNA biogenesis pathway that requires Ago catalysis. *Nature*. 2010; 465: 584–9. DOI: 10.1038/nature09092 [PubMed: 20424607]
28. Chandrass SD, Schirle NT, Szczepaniak M, MacRae IJ, Joo C. A Dynamic Search Process Underlies MicroRNA Targeting. *Cell*. 2015; 162: 96–107. DOI: 10.1016/j.cell.2015.06.032 [PubMed: 26140593]
29. Schirle NT, Sheu-Gruttadauria J, MacRae IJ. Gene regulation. Structural basis for microRNA targeting. *Science*. 2014; 346: 608–13. DOI: 10.1126/science.1258040 [PubMed: 25359968]
30. Parker JS. How to slice: snapshots of Argonaute in action. *Silence*. 2010; 1: 3. doi: 10.1186/1758-907X-1-3 [PubMed: 20226069]
31. Wagner M, et al. Expanding and understanding the genetic toolbox of the hyperthermophilic genus *Sulfolobus*. *Biochemical Society transactions*. 2009; 37: 97–101. [PubMed: 19143610]
32. Brock TD, Brock KM, Belly RT, Weiss RL. *Sulfolobus*: a new genus of sulfur-oxidizing bacteria living at low pH and high temperature. *Archiv fur Mikrobiologie*. 1972; 84: 54–68. [PubMed: 4559703]
33. Berkner S, Wlodkowski A, Albers SV, Lipps G. Inducible and constitutive promoters for genetic systems in *Sulfolobus acidocaldarius*. *Extremophiles : life under extreme conditions*. 2010; 14: 249–59. DOI: 10.1007/s00792-010-0304-9 [PubMed: 20221889]
34. Wagner M, et al. Versatile Genetic Tool Box for the Crenarchaeote *Sulfolobus acidocaldarius*. *Frontiers in microbiology*. 2012; 3: 214. doi: 10.3389/fmicb.2012.00214 [PubMed: 22707949]
35. Rachel R, et al. Analysis of the ultrastructure of archaea by electron microscopy. *Methods in cell biology*. 2010; 96: 47–69. [PubMed: 20869518]

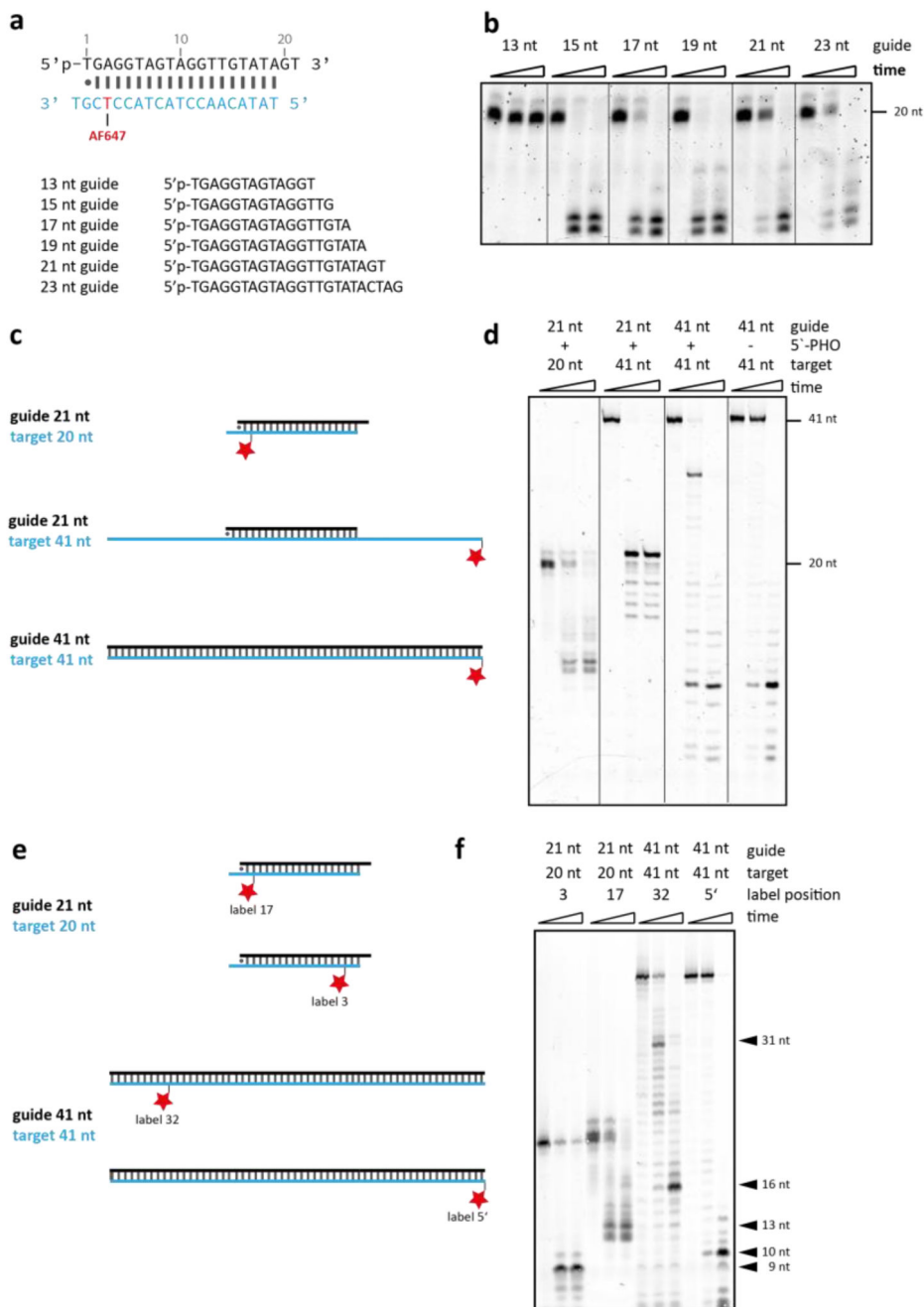


Figure 1. Guide-directed target cleavage activity of MjAgo using canonical and non-canonical substrates.

(a) Guide and target strand sequences used are derived from the human let-7 miRNA and are shown as DNA duplex, which is efficiently cleaved by MjAgo (the Alexa647 (AF647) modification site in the target strand is highlighted in red)¹¹. (b) Different guide strand lengths (13-23 nt) were used for cleavage reactions (3 μ M MjAgo, 1.7 μ M DNA_{guide} and 0.72 μ M DNA_{target} at 85°C) and the reactions were stopped after 0, 7.5 and 15 min. Cleavage products were resolved on a 12% denaturing polyacrylamide gel. Efficient target

strand cleavage requires a minimal guide length of 15 nt. **(c)** Canonical and non-canonical substrates (composed of long guide and long target strands) were used for MjAgo cleavage reactions (fluorophore coupling site is indicated by a red star). **(d)** MjAgo cleaves all offered DNA substrates even when an overlong guide strand of 41 nt is used (0.6 μM MjAgo, 1.7 μM DNA_{guide} and 0.72 μM DNA_{target} at 85°C, time points: 0,15, 20 min). **(e)** Substrates with a fluorescent marker dye positioned either at the 5' or 3' end of the target of a short or long ds DNA substrate. **(f)** MjAgo mediated cleavage pattern of non-canonical substrates shown in **(e)** reveal a stepwise processing of the DNA from the 5'-end of the target. Each experiment was carried out at least three times as biological replicate and a representative gel is shown.

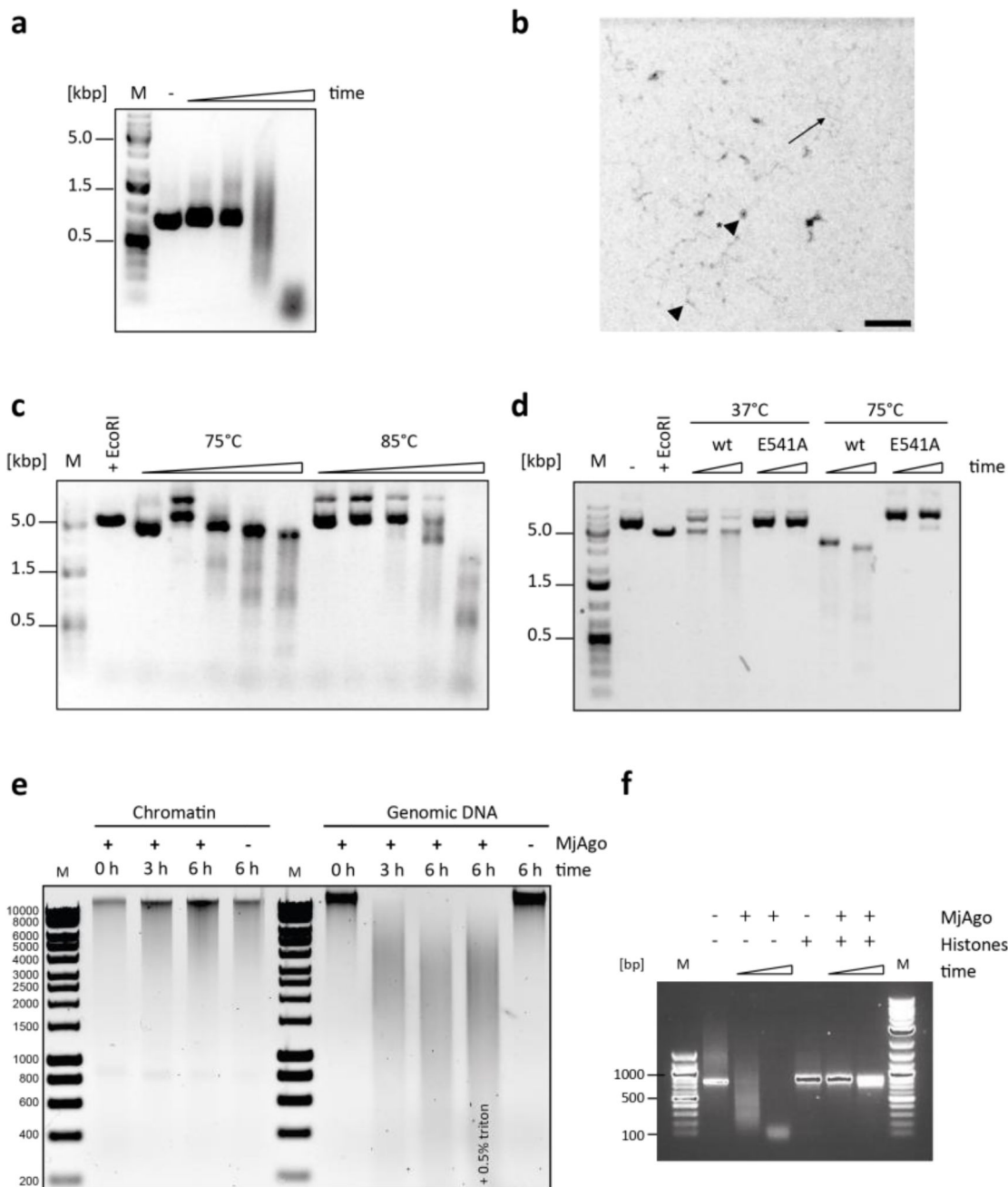


Figure 2. MjAgo processes long linear and circular double-stranded DNAs and genomic DNA in the absence of a guide DNA.

(a) MjAgo mediated cleavage of linear dsDNA (1.1 μ M MjAgo, 1 μ g PCR product at 85°C, time points: 15, 30, 60, 120 min). (b) Transmission electron microscopy (TEM) image of a MjAgo-linear dsDNA sample. Filled arrowheads show proteins associated with dsDNA indicates standard arrows point to naked dsDNA. Scale bar: 100 nm. (c) Time-course of MjAgo-mediated processing of circular plasmid DNA in the absence of DNA guides at 75°C and 85°C (1 μ M MjAgo, 1 μ g plasmid DNA; time points for cleavage at 75°C: 0, 1,

2, 4, 6h; time points for cleavage at 85°C: 0, 2.5, 10, 30, 60 min). (d) Comparison of the wildtype (wt) and a catalytic mutant of MjAgo (E541A) in the plasmid DNA cleavage assay at 37°C and 75°C (1 µM MjAgo, 1.1 µg plasmid DNA, time points: 3 and 6 h; - : untreated plasmid DNA, + EcoRI: EcoRI digested plasmid). (e) Agarose gel electrophoresis of *M. jannaschii* chromatin and *M. jannaschii* genomic DNA after incubation with MjAgo (7.5 µM MjAgo, 37.7 ng chromatin or 780 ng genomic DNA at 37°C). Sample containing 0.5% triton is a control reaction as the chromatinised DNA was prepared in a buffer containing 0.5% triton. (f) Cleavage reaction using linear dsDNA (750 bp) in the presence and absence of *M. jannaschii* histone A3. 1.5 µg dsDNA fragment was incubated with 1 µM MjAgo at 85°C. Samples were taken after 45 and 90 min of incubation and resolved on a 1% Agarose gel. MjAgo mediated degradation is clearly visible in the absence of histones. If the dsDNA is pre-incubated with 14.3 µM *M. jannaschii* histone A3, the DNA is protected against MjAgo degradation (time points 0, 45, 90 min). Experiments in panels a,c-f were carried out at least three times as biological replicate and a representative gel is shown. Experiment in panel B was carried out two times as biological replicate and a representative image is shown.

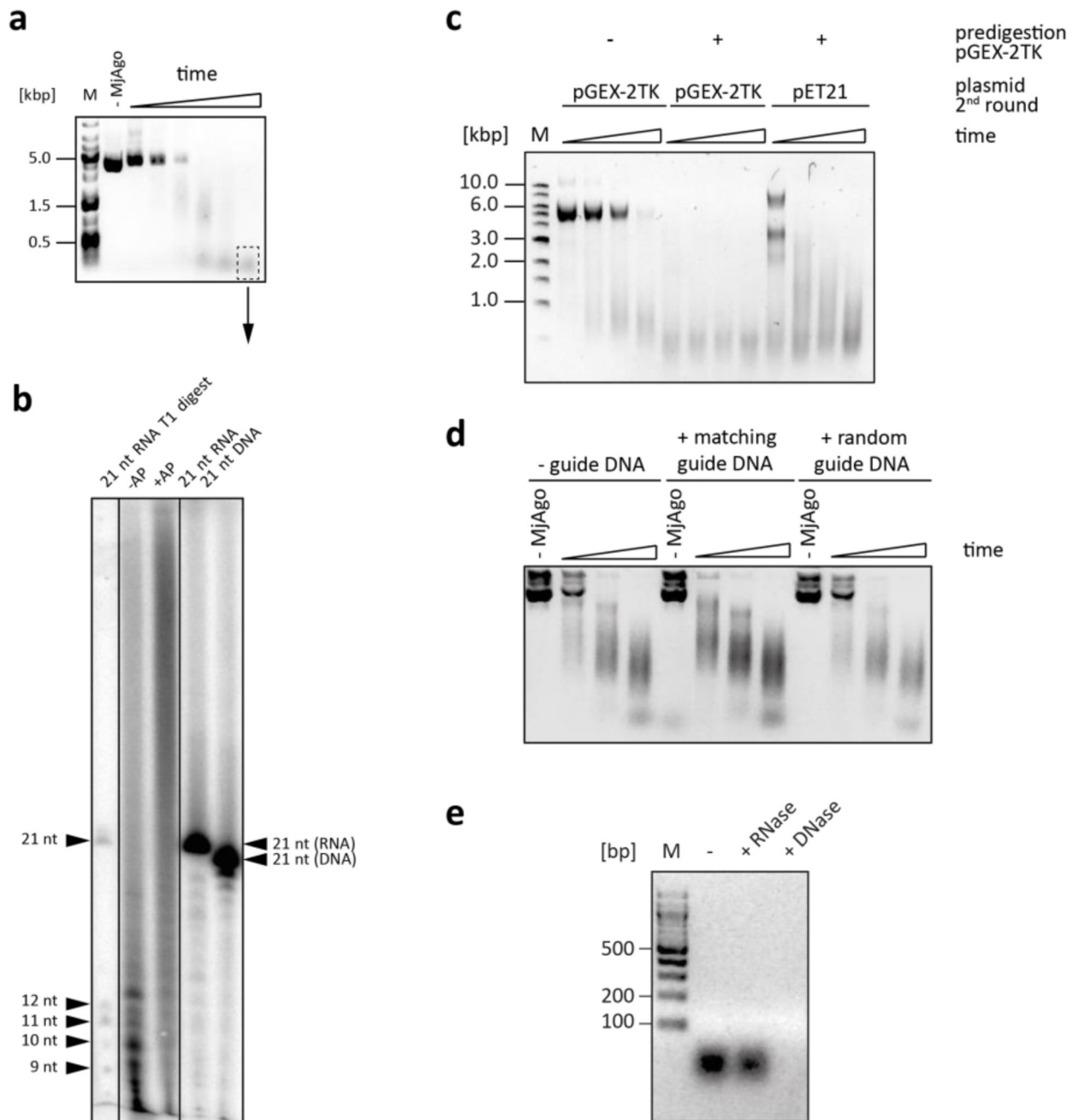


Figure 3. Characterisation of DNA degradation products and influence on MjAgo-mediated plasmid degradation.

(a) Final degradation products of a MjAgo-mediated plasmid DNA degradation that has run to completion (1 μ M MjAgo, 1 μ g plasmid DNA, 85°C, time points: 0, 2.5, 10, 30, 60, 180 min). (b) Final degradation products were extracted, radiolabelled and separated on a 20% denaturing sequencing polyacrylamide gel. (c) 1 μ g pGEX-2TK plasmid was digested to completion with MjAgo (2 μ M MjAgo, 2h at 85°C). Subsequently, a fresh aliquot of the same plasmid (1 μ g pGEX-2TK) or a plasmid with a different sequence (pET21-derived

plasmid) was added to start a new round of cleavage reaction (2 μ M MjAgo, 1 μ g plasmid DNA at 85°C, time points: 0, 5, 10, 20 min). **(d)** Agarose gel electrophoresis analysis of plasmid DNA incubated with MjAgo in the absence of guide DNA strands (- guide DNA), with MjAgo in the presence of two matching 5'-phosphorylated guides that target each strand of the T7 promoter sequence in the pET-vector, respectively (+ matching guide DNA). In addition, MjAgo in the presence of random non-matching guide DNA was used. Reactions contained 1 μ M MjAgo, 600 ng pET plasmid DNA and were incubated for 0, 15, 30 and 60 min at 37°C. **(e)** Agarose gel electrophoresis of co-purified nucleic acids extracted from affinity purified MjAgo (purification at 4°C) after heterologous expression in *E.coli*. Nucleic acids were Phenol/Chloroform extracted from the protein and digested with the nucleases given. Experiments in panels **a,c-f** were carried out at least three times as biological replicate and a representative gel is shown. Experiment in panel **B** was carried out three times as technical replicate and a representative image is shown.

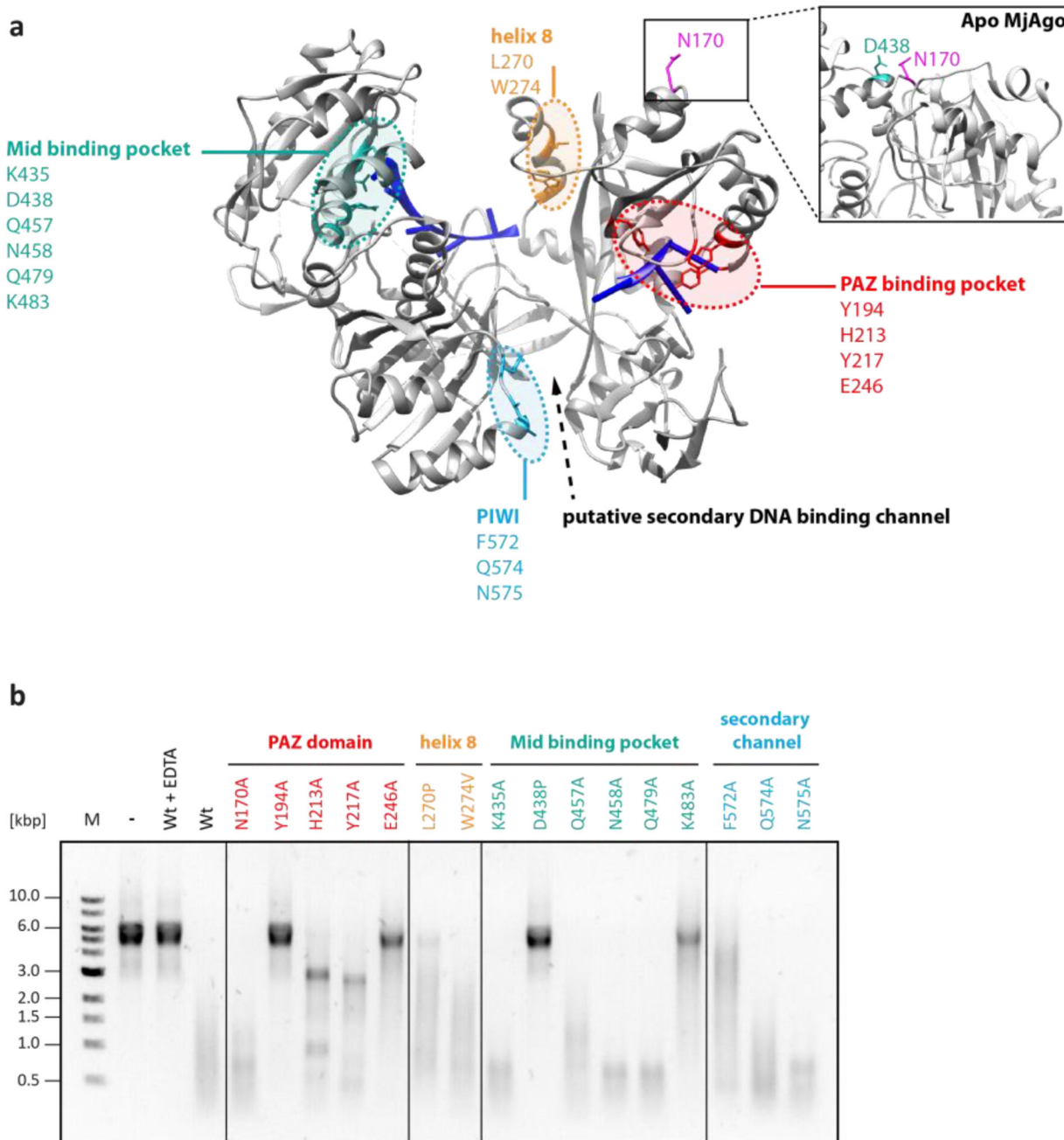


Figure 4. Mutational analysis of MjAgo guide-independent plasmid cleavage activity.

(a) MjAgo crystal structure in complex with a 21 nucleotide guide strand (PDB: 5G5T). The 5'-end of the guide is anchored in the Mid domain binding pocket (highlighted in teal), the 3'-end is bound in the PAZ domain binding pocket (red). Helix 7 is a flexible element (orange) that undergoes conformational changes and is involved in correct positioning of a target strand (see also Figure S7). MjAgo structures revealed the position of a putative third nucleic acid binding channel (light blue) located between the PIWI and N-terminal domain. Positions of the MjAgo point mutations used for plasmid cleavage studies are highlighted.

Inset shows the apo MjAgo structure (PDB: 5G5S). Due to a rotation of the PAZ domain, residues N170 and D438 are located in close proximity potentially interacting with each other. **(b)** Agarose gel electrophoreses of the final plasmid degradation products of MjAgo wt and MjAgo mutants (1 μ M MjAgo, 300 ng plasmid DNA; cleavage for 2h at 85°C). As a control, the plasmid was incubated in the absence of MjAgo (-) or with MjAgo wt in the presence of EDTA (wt + EDTA). The experiment was carried out twelve times (including biological as well as technical replicates) and a representative gel is shown.

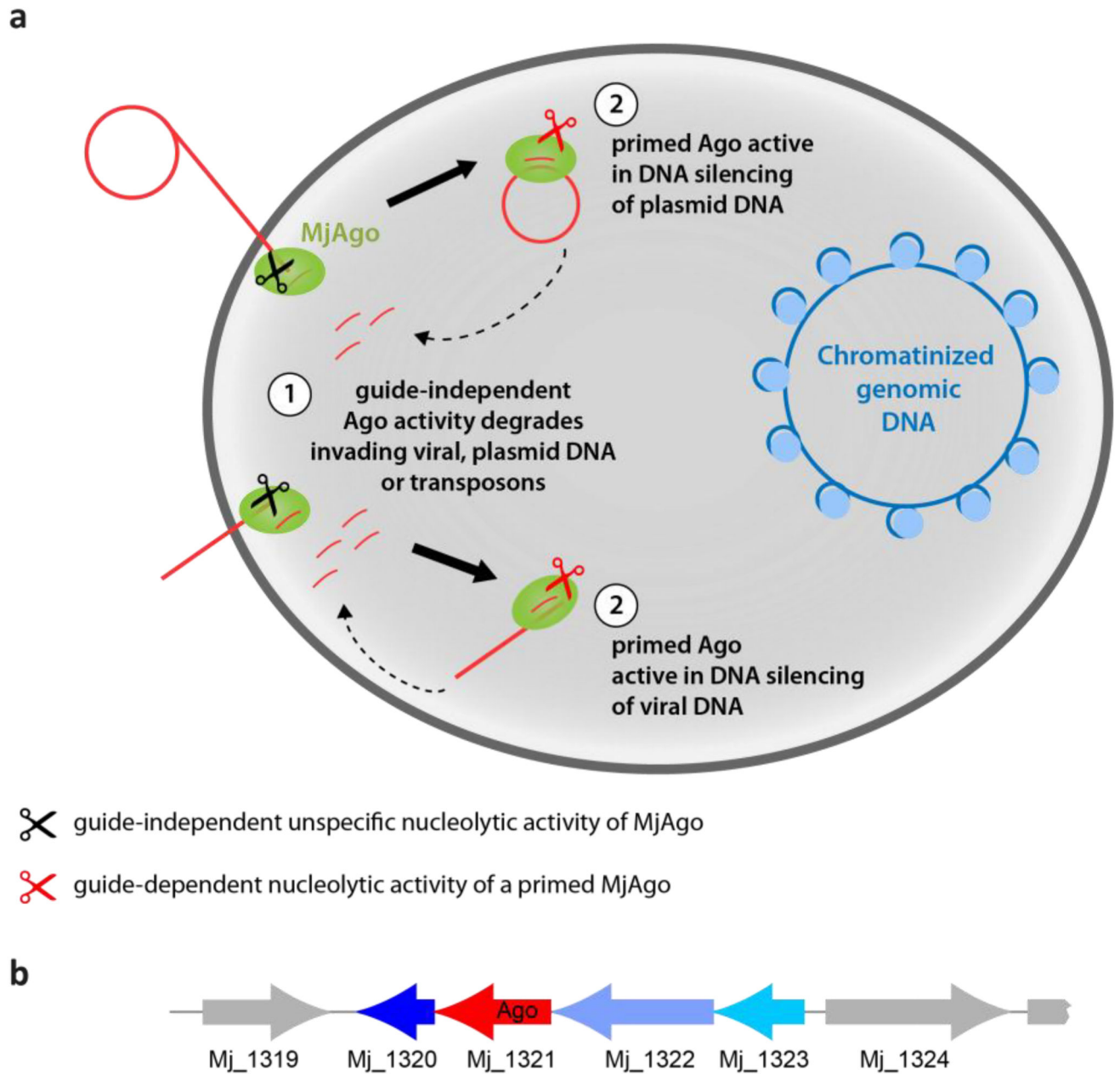


Figure 5. Putative model of guide-dependent and guide-independent DNA silencing by MjAgo. (a) (1) Invading nucleic acids like plasmid DNA or viral DNA are recognised by MjAgo and will be subject to nucleolytic degradation. *M.jannaschii*'s genomic DNA (gDNA) is protected against MjAgo-mediated degradation as *M.jannaschii* encodes histone proteins that keep the gDNA in a chromatinized state. (2) The first round of guide-independent degradation leads to a primed MjAgo with accelerated MjAgo-mediated cleavage of DNA in a second cleavage round. One priming mechanism is the incorporation of short DNA fragments generated during the first wave of DNA degradation. These DNAs can serve as guide to direct guide-dependent silencing of invasive nucleic acids. (b) Genomic location

of MjAgo (Mj_1321). Blast search in the KEGG genome database revealed that MjAgo is encoded in a cluster with three hypothetical proteins, showing similarities to enzymes involved in rRNA processing (Mj_1320, RNase motif) and DNA recombination /repair (Mj_1322: exonuclease SbcC, Mj_1323: DNA repair protein RAD32).